Physico-chemical Studies on Surface Active Agents. (II) : The Coagulation of Positive Silver Iodide Sols by Anionic Surface Active Agents

AUTHOR(S):

Watanabe, Akira

Physico-chemical Studies on Surface Active Agents. (II)

The Coagulation of Positive Silver Iodide Sols by Anionic Surface Active Agents

Akira WATANABE*

(Tachi Laboratory)

Received March 15, 1960

The coagulation kinetics of positive silver iodide sols by anionic surface active agents, *i. e.* alkyl sulphates, sulphonates and an alkyl phosphate, have been studied spectrophotometrically, and the changes in surface potential of the particles by addition of these surface active agents followed by zeta potential measurements using ultra-microelectrophoresis. The stability factors as functions of the surface active agent concentration and of the zeta potential thus obtained were in excellent agreement with the theory of Part 1 and a reasonable value of the van der Waals constant has been obtained. Zeta potentials as functions of surface active agent concentrations were in good agreement with the theoretical treatment of Part 1 over the lower concentration range, and reasonable values of maximum numbers of available sites and free energies for the first layer adsorption have also been estimated. An attempt has been made to interpret the deviation of experimental results from theory at higher concentrations by introducing the concept of second layer adsorption mechanism.

I. INTRODUCTION

In the last paper (Part 1)[1] a theory has been derived relating the stability of a sol to the surface active agent concentration, under conditions such that the ionic strength remains virtually constant. It was found that the stability is governed by the surface potential change which occurs on adsorption of the surface active agent.

It is the purpose of this paper to give an experimental verification of this theory by determining the stability of formed positive silver iodide sols, having a mean particle radius of *ca.* 100 Å, in the presence of alkyl sulphates, sulphonates and an alkyl phosphate.

Although various studies of the influence on sol stability of a number of large organic ions, including strychnine[2,3], morphine[4], guanidine[3], alkyl pyridinium[5,6,7], dodecyl sulphate[6,8,9] and dodecylamine[9], *etc.*, have appeared in the literature, most of this work does not give sufficient data to test the theory in detail. An exception is the recent experimental work of Rastogi[10] on negative silver iodide sols in the presence of cationic surface active agents.

The stability of hydrophobic sols is mainly governed by the magnitude of the potential energy of interaction between the double layers of approaching particles and removal of this energy barrier, by various means, leads to coagulation. Hence, the rate of coagulation may be used as a means of measuring stability and, in

* 渡　辺　　昌

practice, turbidimetric measurements provide an excellent method for determining this rate[11,12,13].

Ideally, to provide a complete test of the theory of Part 1, measurements of the Stern potential, ψ_δ, are required, but at the present time this would not seem a very practical possibility for sol particles; some estimate of this potential can be made from double layer capacity measurements on silver iodide suspensions[14]. Measurements of zeta potential, ζ, however, despite the practical difficulties of interpretation[15] do provide a useful, and readily accessible, measurement of part of the potential drop within the double layer. Moreover, it would appear reasonable to assume that, under certain conditions, particularly near the zero point of charge, ψ_δ and ζ may have the same identity.

From these measurements, therefore, it was hoped to build a successful foundations for the further understanding of the coagulation mechanism as well as of the mode of adsorption of surface active agents in the electrical double layer.

II. EXPERIMENTAL

1. Materials

The silver nitrate and postassium iodide used were of Analar grade and were not purified further. The anionic surface active agents used were, sodium decyl sulphate (SDeS), sodium dodecyl sulphate (SDS), sodium tetradecyl sulphate (STS), sodium dodecyl sulphonate (SDSO), sodium dodecyl benzenesulphonate (SDBSO), sodium dioctyl sulphosuccinate (Manoxol OT), and dodecyl dihydrogen phosphate (DHP). All materials were of high purity (>99.6%).

Ordinary distilled water was passed through a column of Bio-deminrolit ion exchange resin and redistilled from an all Pyrex apparatus; this gave water of specific conductivity 1.04×10^{-6} ohm^{-1} cm^{-1} which was used for all experiments.

All glassware was thoroughly cleaned and steamed before use.

2. Preparation of Sols

The positive silver iodide sol was prepared by adding 200 ml of 10^{-3} M potassium iodide solution to an equal volume of 3×10^{-3} M silver nitrate solution; the solution was vigorously stirred during the addition[10]. The sol prepared, therefore, was of concentration $5\times10^{-4}M$, pAg=3, ionic strength 1.5×10^{-3} M and contained 0.5×10^{-3} M potassium nitrate.

Owing to the asymmetric position of the isoelectric point of silver iodide sols, *e.g. ca.* pAg 6[16], the positive silver iodide sol becomes unstable when electrodialysed. Hence the latter procedure was dispensed with and the sol was kept in a dark room at room temperature for about three hours; after this period the rapid ageing process had ceased and the particle radius had become virtually constant.

The effect of ageing was examined by following the turbidity change with time and also by electron microscopy. The positive silver iodide sol was found to have a lower stability than the negative sol and it was impossible to obtain a stable aged sol by heat treatment. However, it is clear from the curve in Fig. 1 that the optical density of the sol becomes practically constant after 3 or 4 hours. As the optical density change due to coagulation was an order of magnitude or so higher

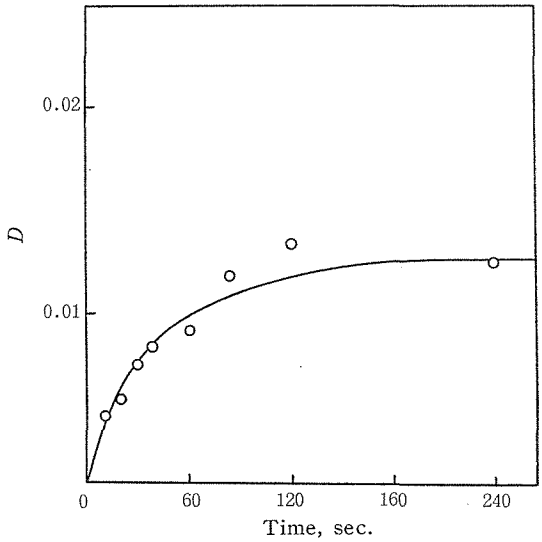

Fig. 1. Optical density *vs.* time after preparation of the positive AgI sol.
AgI sol : $5\times10^{-4}M$, pAg=3

than the order of change on standing, the change in optical density with time on ageing was negligible (after 3 hours), particularly as the observations of coagulation were made in a few seconds. Usually, some coagulation was found to have taken place on 24 hours' standing and therefore the sol was prepared freshly each day and then aged for three hours before use.

Fig. 2 shows the particle size distribution curves after 1 and 60 min as obtained

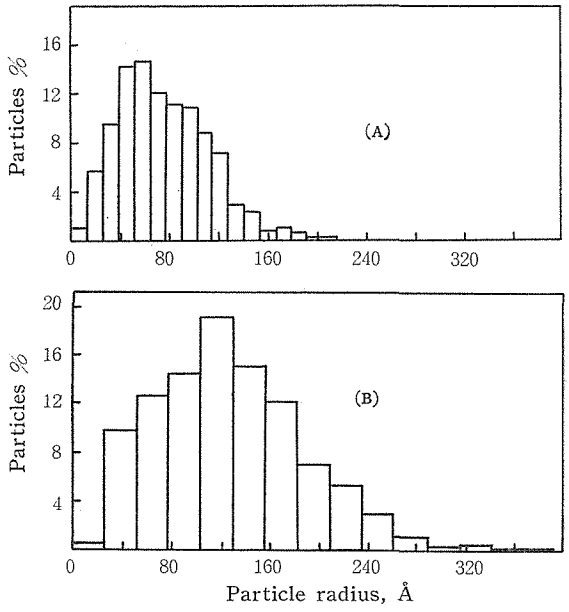

Fig. 2. Particle size distribution of positive AgI sol, pAg=3.
(A) 1 min. after preparation
(B) 60 min. after preparation

from analysis of electron micrographs (Fig. 19). Curves show that the mean particle radius after 60 min was 100Å.

In the special case of experiments at $\tau=\kappa a=3$ [IV, 3, (ii), Fig. 25] the sol was prepared as follows; 100 ml of 2×10^{-3} M potassium iodide solution were added to an equal volume of 6×10^{-3} M silver nitrate solution in the manner previously described. After 3 hours' ageing, 3 ml of 1.5×10^{-2} M potassium nitrate solution was added to an equal volume of this sol 1 min before each measurement. Hence, the final sol concentration and pAg were the same, but κa was 3 instead of 1.23.

3. Methods of Measurements

(i) Turbidity

a. The relation between turbidity and particle size. Turbidity τ' is defined by the Lambert-Beer law, *viz.*

$$I_{tr}=I_{in}\exp(-\tau' l) \tag{1}$$

where I_{in} and I_{tr} are the intensities of the incident and transmitted light respectively, and l is the optical path of the cell used. According to Rayleigh's theory of light-scattering, the turbidity is related to the number of particles per cm^3, N, and their individual volume, V_S, by the relation,

$$\tau'=A_R N V_S^2 \tag{2}$$

with

$$A_R=\frac{24\pi^3 n_0^4}{\lambda^4}\left(\frac{n^2-n_0^2}{n^2+2n_0^2}\right)^2 \tag{3}$$

where n_0 and n are the refractive indices of the solvent and the particle, respectively, and λ is the wave length of the light used, *in vacuo*. These equations hold only for spherical particles with a radius smaller than 0.05λ and in the absence of consumptive light absorption.

b. Calculation of the stability factor. An equation relating the turbidity change as a function of time for a coagulation process has been derived by Troelstra and Kruyt[11] and Oster[17]. As the total turbidity of a dilute sol is the sum of the contributions of particles of various sizes, equation (2) becomes

$$\tau'=A_R\sum_{i=1}^{\infty}N^i(V_S{}^i)^2,$$

where the superscript i refers to the i-fold particle. Substituting equation (22) of Part 1 for the particle distribution at a time t, and considering $V_S{}^i=iV_S$, where V_S is the volume of a primary particle, we obtain

$$\tau'=A_R V_S^2 N_b\sum_{i=1}^{\infty}\frac{i^2(t/T_{tr})^{i-1}}{[1+(t/T_{tr})]^{i+1}}=A_R V_S^2 N_b[1+(2t/T_{tr})] \tag{4}$$

Differentiating with respect to t, we obtain

$$d\tau'/dt=8\pi\mathcal{D}R(V_S N_b)^2 A_R/W \tag{5}$$

where equation (21) of Part 1 has been used. Equations (4) and (5) apply only to the initial stages of coagulation. They show that the turbidity changes linearly with

time and that the initial slope is proportional to the square of the sol concentration and inversely proportional to the stability factor, W.

If the sol concentration is expressed by c_s in g cm^{-3}, equation (5) reads

$$d\tau'/dt = k' c_S^2/W$$

or $$\log W = \log (dt/dD) - \log (2.303/k' c_S^2) \quad (6)$$

where $$k' = A_R k_0/d^2 \qquad g^{-2}\ cm^5\ sec^{-1} \quad (7)$$

and $$k_0 = 8\pi \mathcal{D} R = 8kT/3\eta \qquad cm^3\ sec^{-1} \quad (8)$$

Here we have introduced the optical density D, which is related to the turbidity by the relation

$$\tau' = 2.303D \quad (9)$$

c. Apparatus. Measurements of optical density were carried out using a Unicam SP 600 spectrophotometer. The change in light transmission with time was followed by an automatic recording system connected to the output of the photometer after a one stage D. C. amplification[12]. The time constant of response of this system was of the order of 1 sec, which was sufficiently small for the present purpose.

Rapid mixing was achieved by a device described earlier[10]. Aliquots of solution of coagulating agents, *e. g.* inorganic salts or surface active agents, in the mixer were added to 3 ml of the positive silver iodide sol in the optical cell (1 cm path length). All measurements were carried out at room temperature (20±1°C) and a wave length of 5460Å (mercury green); at this wave length no consumptive light absorption occurs.

(ii) Microelectrophoresis

a. Apparatus. Electrophoretic measurements were carried out using an apparatus based on the design of van Gils and Kruyt[18,19]. The cell consisted of a thin cylindrical Pyrex glass capillary of inner radius 1.185 mm and of wall thickness 0.160 mm. The electrodes were platinised platinum set about 5 cm apart. A constant voltage of 15 volts was applied across them. Under these conditions, which were normally employed, a field strength of 2.44 volt cm^{-1} was obtained. The latter was determined from the current passing through the cell when it was filled with a standard 10^{-3} M silver nitrate solution (specific conductivity 0.00012 ohm^{-1} cm^{-1}). It was found effective to short-circuit the electrodes during a resting period in order to ensure depolarisation. All measurements were carried out at room temperature (20±1°C).

b. Fluoride treatment of the cell. According to Davies and Holliday[20], the mobility of positive silver bromide particles is strongly influenced by the silicate ions dissolved from the glass wall of the cell. In order to obtain reproducible mobility measurements, these authors washed the cell with hydrofluoric acid; this treatment converts the soluble silicate ions of the cell surface into insoluble fluosilicate ions.

As a similar situation appears to occur in the case of positive silver iodide sols, the following treatment was made before each series of mobility measurements on one kind of surface active agent: after washing with about 200 ml of warm distilled

water, the whole cell was filled with an approximately 10^{-3} M sodium fluoride solution which contained a small amount of hydrofluoric acid, *i. e.* the solution was adjusted to pH 3.5. After standing for about 30 min, the cell was washed thoroughly with about 1 litre of distilled water.

c. Optical correction. The calculation of the optical effect due to the refraction of the incident light beam at the glass-liquid interfaces had been made by Rastogi[10]. It was found that the correction factor was negligible in the case of a cylindrical cell of thin glass placed in a water bath.

d. Stationary level. When electrophoresis is carried out in a glass cell, there is always in addition electro-osmosis. This is due to the fact that the glass wall is negatively charged with respect to the water. The electro-osmotic flow is superimposed on the electrophoretic movement of the particle. For a cylindrical cell of inner radius r_w, the following relation holds between the apparent velocity observed microscopically, U_{app}, and the true electrophoretic mobility, U,

$$U_{app}=U+U_{osm}[(2r^2/r_w^2)-1] \tag{10}$$

where r is the distance from the axis of the cylindrical cell and U_{osm} the electro-osmotic velocity of liquid at the inner surface of the wall ($r=r_w$). Fig. 3 shows

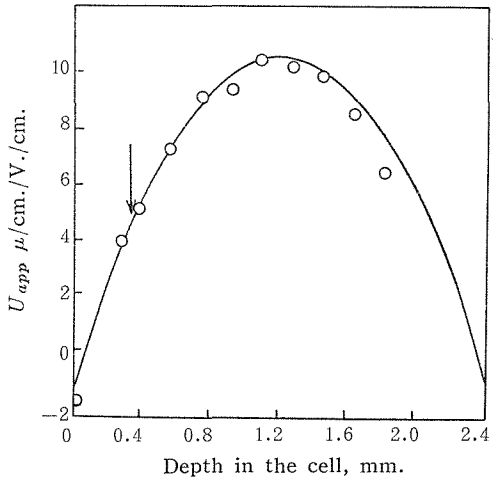

Fig. 3. Observed and calculated mobilities of positive AgI particles, pAg=3, at different depths in the cell.
○ Experimental — Calculated ↓ Stationary level

the parabolic plot of U_{app} *vs.* r obtained by an experiment on a positive silver iodide sol (pAg 3). The theoretical curve was obtained by substituting in equation (10) the values 4.7 and 0.56 μ/sec/volt/cm for U and U_{osm}, respectively; these values were calculated from the linear plot of U_{app} *vs.* $[(2r^2/r_w^2)-1]$ of experimental data.

It is clear from equation (10) that $U_{app}=U$ for $r=r_w/\sqrt{2}$, and this position is called the "stationary level". The mobility at the stationary level should not change even if U_{osm} is changed due to the change in ζ potential of the glass wall. It has been checked experimentally that, even though such a change in U_{osm} occurred in the experiments carried out on silver iodide particles in the presence of anionic

surface active agents, the velocity distribution at different levels in the cell maintained the parabolic shape. We can conclude, therefore, that, provided mobility measurements are carried out always at the stationary level, the mobility values obtained are not influenced by changes on the glass wall.

e. Mobility measurements. Measurements were made at the stationary level and at two other levels in order that the value at the stationary level could be checked by interpolation. The mobility values used for the calculation of ζ potential were the average of twenty readings of the particle velocities; the polarity of the applied potential was reversed for each set of readings.

The accuracy of the mobility varied according to conditions. In some cases a change with time was observed, either due to coagulation or to slow adsorption of surface active agents.

f. Calculations of ζ Potential. The ζ potential was calculated from the observed mobility using the Overbeek formula[21] which includes corrections for relaxation and the Henry effect. For an insulating particle in a symmetrical $v-v$ valent electrolyte solution, this equation reads

$$U=(e\zeta/6\pi\eta)\,\mathrm{f}\,(\kappa a,\zeta) \tag{11}$$

where

$$\mathrm{f}(\kappa a,\zeta)=\mathrm{f}_1(\kappa a)-v^2(e\zeta/kT)^2\,\mathrm{f}_3(\kappa a) - [(\rho'_+ + \rho'_-)/2e](\varepsilon\, kT/6\pi\eta e)(e\zeta/kT)^2\,\mathrm{f}_4(\kappa a) \tag{12}$$

ρ'_+ and ρ'_- are the frictional constants of the cation and anion of the electrolyte, respectively, and $\mathrm{f}_1(\kappa a)$, $\mathrm{f}_3(\kappa a)$ and $\mathrm{f}_4(\kappa a)$ are characteristic functions defined by Overbeek.

In calculating the correction function, $\mathrm{f}(\kappa a,\zeta)$, the values of ρ'_+ and ρ'_- are not critical provided that normal ions are predominant; the values taken were based on an ionic mobility of 70 $\mathrm{ohm^{-1}\ cm^{-1}}$ for all ions. The values of ε and η were assumed to be the same as water ($\varepsilon=80$ and $\eta=0.01$ poise), because in almost all cases the concentrations of the various ionic species, including the surface active ions, were less than 1.5×10^{-3} *M*. The ionic strength of the sol was usually $1.5\times10^{-3}M$, and hence, assuming $a=100$Å, $\kappa a=1.23$. Unfortunately, it is for sol particles in this region of κa values where the relaxation correction becomes most important.

Although the Overbeek formula was derived by assuming $e\zeta/kT\ll1$, or $\zeta\ll25$ mV for $v=1$, the values of ζ obtained were often larger than 100 mV. Recently, a more accurate calculation has been made by Wiersma[22]; this author, using the complete form of the Debye-Hückel equation, has shown that the correction function (12) applied to ζ potential values of less than 100 mV with negligible errors.

(iii) Electron Micrographs

Micrographs were taken using a Siemens Elmiskop I, which has been shown to be capable of resolving silver iodide particles of less than 10 Å[23]. Micrographs were usually taken at magnifications of ×8,000 or ×40,000.

Samples were removed by means of a small platinum loop and droplets deposited on to carbon films mounted on copper supporting grids.

III. RESULTS

1. Measurement of Stability by Turbidimetry

(i) Coagulation of Positive Silver Iodide Sols by Inorganic Ions

Before working with surface active agents some preliminary experiments were carried out with inorganic anions to test the validity of the method and the cacu-lation of the absolute value of W. It is important to point out here that equations (4) to (9) are general for the early stage of coagulation, as far as the fundamental diffusion equation holds; that is, they are valid independent of whether coagulation is due to a change of ψ_δ or of τ.

a. Optical density *vs.* time curves. Fig. 4 shows typical curves of optical density *vs.* time obtained by adding sodium sulphate to a positive silver iodide sol. It is clear from these curves that the initial portions are sufficiently linear to be in agreement with theoretical expectations, *vide* equations (4) and (5).

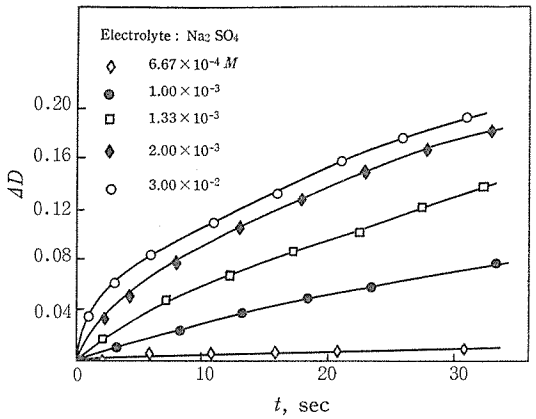

Fig. 4. Δ Optical density *vs.* time for coagulation of Ag I sols by sodium sulphate.
Ag I sol : 5×10^{-4} M, pAg=3.

b. Log (dt/dD) *vs.* log c_e curves. According to the theory of Reerink and Overbeek[13] in which the effect of the change of τ on coagulation is treated, a linear relationship holds between log W and log c_e in the slow coagulation range, where c_e is the electrolyte concentration in moles per litre, *i. e.*

$$\log W = -(A/24u_m kT)\log c_e - (A/24u_m kT) \times \log (8\pi \mathrm{N} v^2 e^2 a^2 10^{-6}/\varepsilon kT) + (3/2 - A/12u_m kT)\log u_m + (1/2)\log 96\pi kT/A \quad (13)$$

where u_m is the value of u giving maximum potential energy of interaction, V, N the Avogadro number, v the valency of the added counter ion, and the other symbols have the same meanings as in Part I[1]. Combining this with equation (6), we can also expect a linear relationship between log (dt/dD) and log c_e.

In Fig. 5 the plots of log $(dt/dD)_{t\to0}$ *vs.* log c_e for various electrolytes are given. In the case of uni- and divalent anions, *i. e.* nitrate and sulphate ions, the

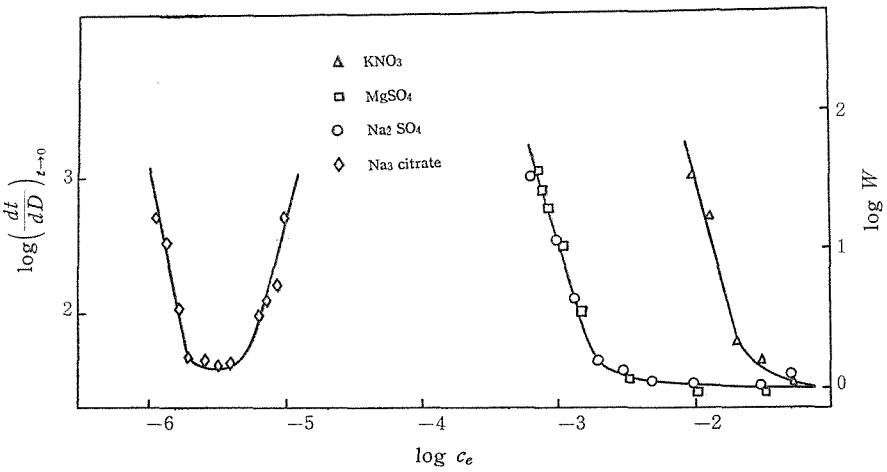

Fig. 5. Coagulation of positive Ag I sol by electrolytes.
AgI sol: 5×10^{-4} *M*, *p*Ag=3.

curves obtained are of the form predicted by the theory; they are linear in the slow coagulation range and become parallel to the abscissa in the rapid coagulation range. In order to show that the coagulation is mainly brought about by the negative ions in the case of a positive silver iodide sol, *i. e.* by the *gegen* (counter) rather than the *neben* ion, plots of curves obtained using magnesium and manganese sulphates in addition to sodium sulphate were also made. It is clear that the coagulation process is independent of the cationic species in this case.

The curve of the trivalent citrate ion has a different shape; instead of becoming parallel to the abscissa, the stability increases again at higher concentrations. The electrophoretic measurements showed that this was due to the reversal of the particle charge which occurred on combining such high valent anions with the positive silver iodide particle surfaces. Hence, the coagulation process must be similar in nature to that caused by anionic surface active agents; it is not simply due to compression of the double layer. Whereas, in the coagulation of negative silver iodide sols by addition of the positive trivalent lanthanum ion, the log *W vs.* log c_e curve obtained was typical to that due to double layer compression. It would seem that this difference can be explained by the larger polarisability, and hence greater adsorbability, of the citrate ion.

c. The absolute value of *W*. If we assume, following Reerink and Overbeek[13], that the portion of the log (dt/dD) *vs.* log c_e curves which is parallel to the abscissa corresponds to rapid coagulation, we obtain from the experimental value of log $(dt/dD)=1.46$ for $W=1$ the following relation:

$$\log W=\log (dt/dD)-1.46 \qquad (14)$$

This relation has been used to convert experimental data (dt/dD) into the theoretically analysable quantity, *W*.

The numerical constant in equation (14) can be compared with the corresponding term in equation (6). Substituting $c_s=5\times10^{-4}$ *M*/litre $=1.175\times10^{-4}$ g/ml, we obtain $k'=5.8\times10^{6}$ g^{-2} cm^{5} sec^{-1}. If we substitute this value of k' in equation (7) together with $A_R=3.70\times10^{19}$ cm^{-4}, which is obtained from equation (3) for $n=2.22$, $n_0=1.33$,

$d=5.67$ g cm^{-3} and $\lambda=5.46\times10^{-5}$ cm, we obtain $k_0=5.04\times10^{-12}$ cm^3 sec^{-1}. On the other hand, the theoretical value of k_0 obtained from equation (8), by taking $k=1.38\times10^{-16}$ erg deg^{-1}, $T=293$ deg and $\eta=0.01$ g cm^{-1} sec^{-1}, is 10.8×10^{-12} cm^3 sec^{-1}. Agreement between these experimental and theoretical values of k_0 is sufficiently good to justify the constant in equation (14).

d. Coagulation concentration. The coagulation concentrations defined by extrapolating the linear portion of the log W *vs.* log c_e curves to log $W=0$ are listed in Table 1. The extremely low value of the citrate ion is a clear indication that the coagulation mechanism is different from the other two cases, since theoretically for a Schulze-Hardy coagulation it should be of the order of $10^{-4}M$[5].

Table 1. Coagulation of positive silver iodide sols by inorganic anions.

Anion	Coagulation concentration M/litre
NO_3^-	2.46×10^{-2}
SO_4^{--}	2.14×10^{-3}
citrate^{---}	2.24×10^{-6}

(ii) Coagulation of Positive Silver Iodide Sols by Anionic Surface Active Agents

a. Optical density *vs.* time curves. The changes of optical density with time which occurred after addition of various long chain sulphates and sulphonates to the sols are shown in Fig. 6 and 7. The early portions of the curves are usually sufficiently linear to enable the initial slopes to be obtained. However, it would appear

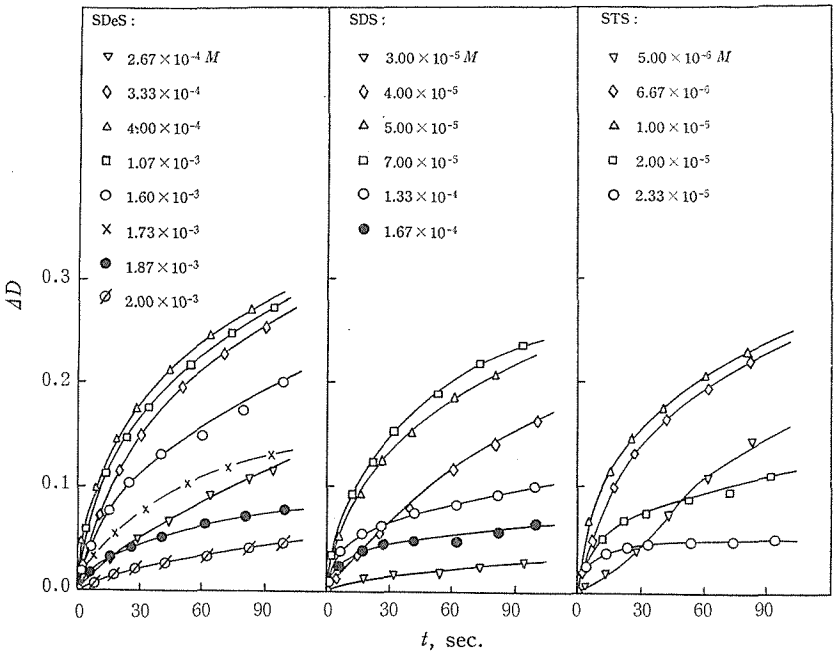

Fig. 6. Δ Optical density *vs.* time for the coagulation of Ag I sols by alkyl sulphates.

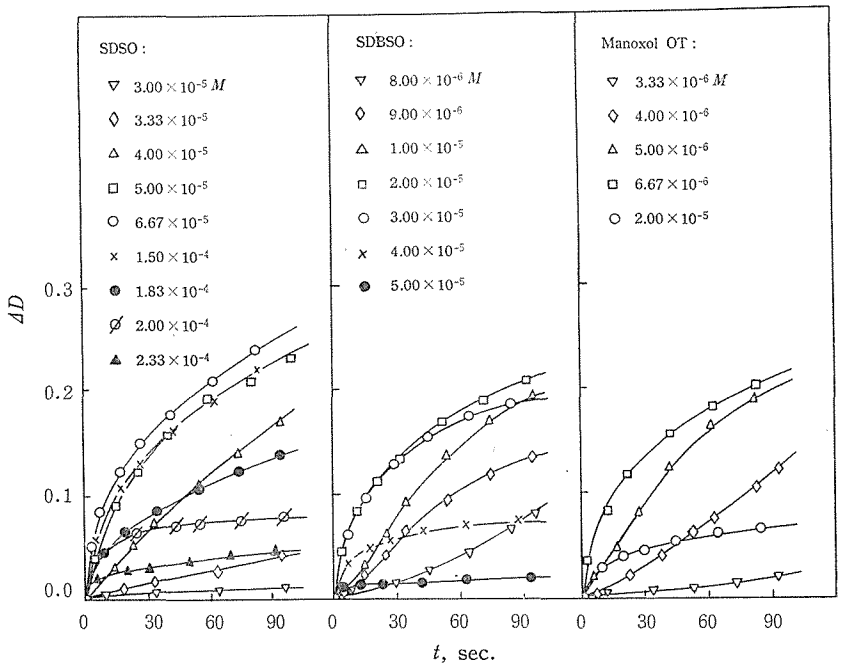

Fig. 7. Δ Optical density *vs.* time for the coagulation of Ag I sols by surface active sulphonates.

on close inspection that linear curves are not always obtained.

A noticeable phenomenon is that in almost every case, except with SDeS and SDS, some sigmoid curves are obtained; this is suggestive of some type of "auto-catalytic" mechanism. Generally, it was found that this type of curve was obtained only in the range of slow coagulation at surface active agent concentrations lower than those required to give rapid coagulation. Moreover, the shape of the sigmoid curve was found to depend on the extent to which the sol had aged. Some examples

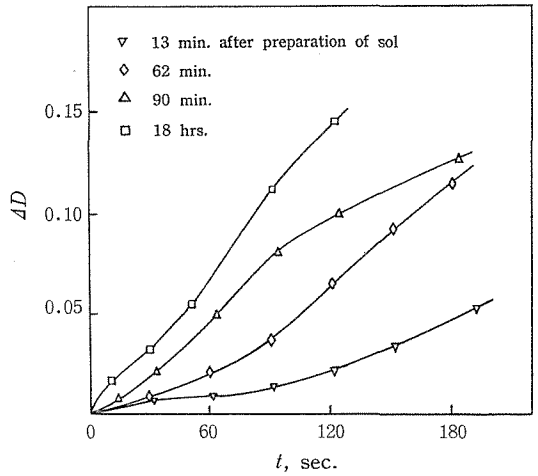

Fig. 8. Δ Optical density *vs.* time for coagulation of positive Ag I sol by SDBSO at different stage of ageing.
Ag I sol : $10^{-3}M$, pAg=3.

are shown in Fig. 8, in which the optical density *vs.* time curves for coagulation of a sol, on addition of SDBSO ($8\times10^{-6}M$), at 13, 62, 92 min and 18 hours after the preparation of the sol, are given. It is clear that the induction time is shorter for the more aged sol.

b. Log *W* *vs.* log *c* curves. The stability factor, *W*, was calculated from the initial slope of the optical density *vs.* time curve by using equation (14); the value of the initial slope was obtained from the increase of optical density 1 sec after mixing in the case of the normal curves, and from the slope of the linear portion of the second stage of the curves in the case of the sigmoid type (see Discussion).

If the values of log *W* thus obtained are plotted against the logarithm of the molar concentration of the surface active agents, we find very marked specificities for these substances. Fig. 9 and 10 show the effects of the chain length for surface active agents with the same head groups, *i. e.* sulphate and sulphonate, respectively, whilst in Fig. 11 the effects of different head groups, *i.e.* sulphate, sulphonate and phosphate (adjusted to *p*H 8.5), for the same alkyl chain, *i.e.* dodecyl, are illustrated.

The general shape of the curves is in good agreement with the theory developed

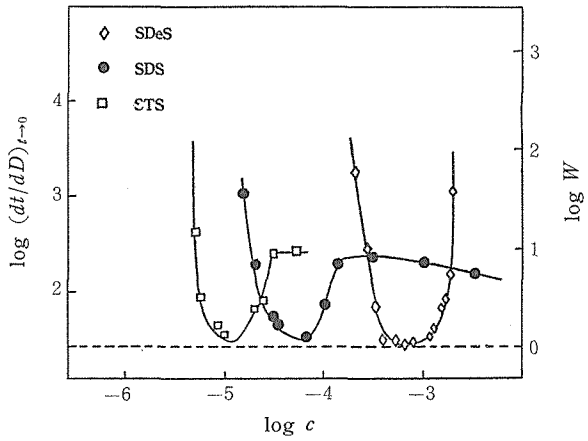

Fig. 9. Log stability *vs.* log molar concn. for alkyl sulphates.

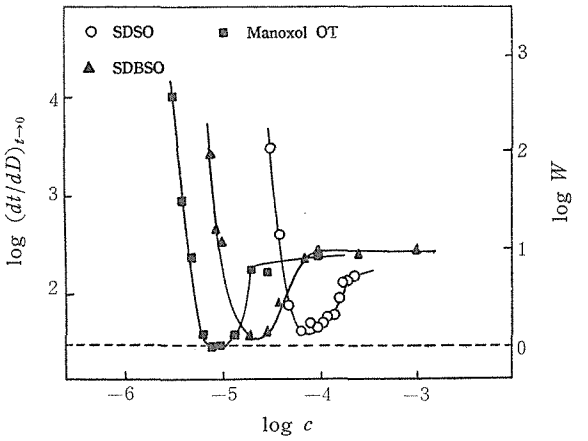

Fig. 10. Log stability *vs.* log molar concn. for surface active sulphonates.

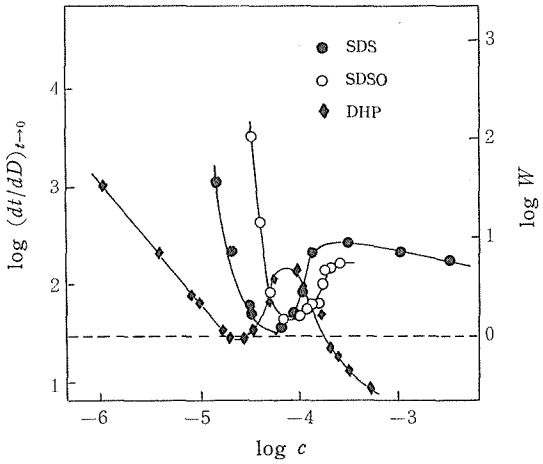

Fig. 11. Log stability *vs.* log molar concn. for dodecyl compounds.

in Part 1[1]. As the surface active agent concentration is increased, the stability decreases and at a certain concentration reaches a minimum value. After this the stability increases again and tends to a certain value (*cf.* Fig. 5 of Part 1).

The effects of chain length are also in good agreement with the theory. The curves corresponding to materials with the same head group have almost the same shape and only the position is shifted. The shift is towards lower concentrations for materials with longer or branched chains (*i. e.* larger values of k_2). On the other hand, the effects of head group differ in the sense that they change the shape as well as the position of the curves. The slope of the curve at concentrations lower than the stability minimum is smaller for sulphate than sulphonate; DHP shows the smallest slope. It is easily seen from a simple consideration of equation (59) in Part 1 that the valency of the surface active agent is also effective, and in fact, DHP will probably be in the form of divalent anion at *p*H 8.5; the values of its first and second pK's are about 2 and 7, respectively[24]. However, the higher charge should increase the stability and the effect observed here is in the opposite sense, *vide* Discussion.

Although the general behaviour of the log W *vs.* log c curves is in good agreement with the theory, a few points arise which it does not explain. In the first place, the limiting values of stability at higher concentrations are always much smaller than the value predicted from the theory (log $W \cong 6$). Moreover, above a certain concentration the stability starts to decrease again with increasing concentration of surface active agents. It seems that this type of deviation from the theory occurs with almost every surface active agent and suggests that the mechanism of coagulation changes at the higher concentrations.

The marked decrease in stability at higher concentrations in the case of DHP is a rather exceptional case. It has been proved experimentally that reaction between the phosphate and the free silver ions originally present in the sol produces a new sol of AgDHP. Hence, this causes an extra optical density increase and the apparent value of log W decreases at higher concentrations. A reaction of this type was proved not to occur with the other surface active agents over the concentration

range in which these experiments were performed.

Another deviation from the theory is the fact that the minimum value of log W is not always zero. It will be shown later that this appears to be intimately related to the deviation of the stability minimum from the zero point of ζ (see Discussion).

c. Coagulation concentration. An alternative method of presentation of the data obtained from coagulation experiments is to plot the optical densities at different times, say 30, 60, 90 and 120 sec, after mixing, against the logarithm of molar concentration of surface active agents[25,26]. This has the advantage of giving a clearer impression of the changes occurring with time. An example is shown in Fig. 12 for coagulation by STS. It has been found that extrapolation of the steepest por-

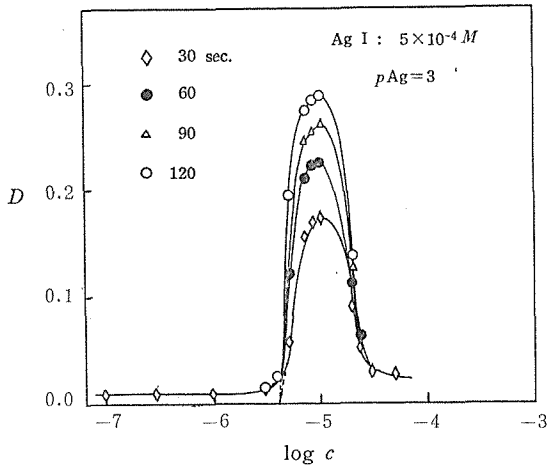

Fig. 12. Coagulation of formed Ag I sol by STS.

tion of the left hand side of the curves for different times usually gives an intersection on the log concentration axis at the same point for a given surface active agent. This fact was also found by Matijević and Ottewill[25] for sol formation in the presence of surface active agent; these authors defined the coagulation concentration by this method. On the basis of the log W *vs.* log c_e curves we had defined the coagulation concentration as the point where the extrapolated initial portion of the curve cut the log $W=0$ axis. Fundamentally, these definitions are the same in principle since the greatest change of optical density occurs in the transition region between slow and rapid coagulation, but, in practice, the actual coagulation concentrations obtained by the two procedures may differ slightly. Thirdly, we can define the coagulation concentration in "adsorption coagulation" as the minimum point of the log W *vs.* log c curve; this definition, however, may be difficult to interpret precisely in cases where a broad coagulation range is obtained. In Table 2 are listed the values of the coagulation concentration obtained by each of the three definitions. Although the values are all of the same order of magnitude, it is clear that each definition gives a different coagulation concentration.

In Fig. 13, 14 and 15 the optical densities at 90 sec after mixing are plotted against the logarithm of molar concentration of surface active agents. The first two

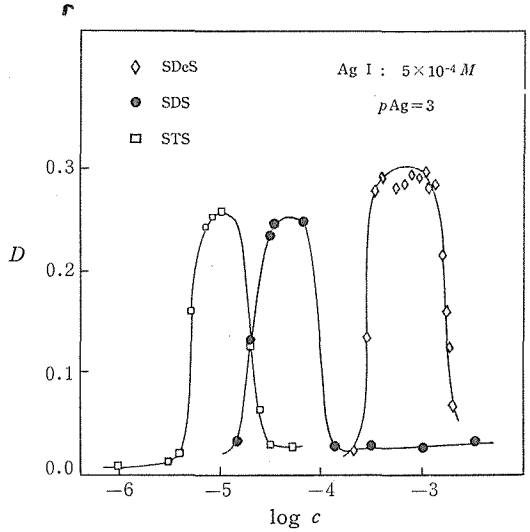

Fig. 13. Optical density, 90 sec. after mixing, *vs.* log molar concn.

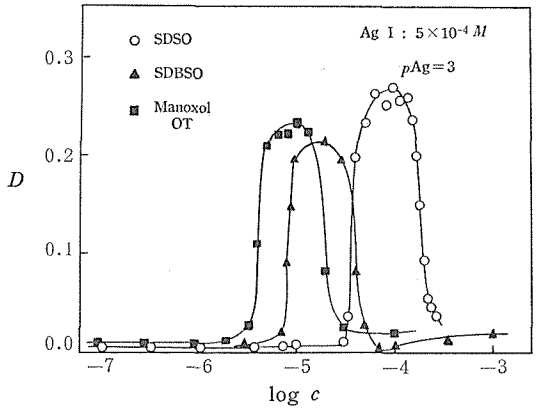

Fig. 14. Optical density, 90 sec. after mixing, *vs.* log molar concn.

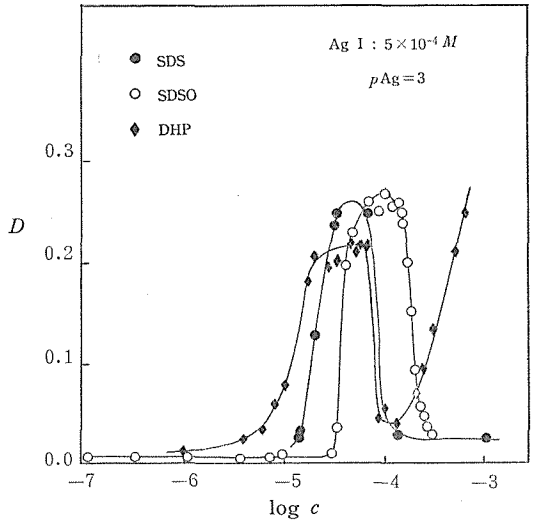

Fig. 15. Optical density, 90 sec. after mixing, *vs.* log molar concn.

figures show the effect of chain length in the case of surface active agents with the same head groups, *i. e.* sulphate and sulphonate, respectively, and the last figure shows the effect of different head groups in the case of surface active agents having the same chain length.

Table 2. Coagulation of positive silver iodide sols by anionic surface active agents

Surface active agent	Coagulation concentration (M)		
	Extrapolation to log $W=0$	Minimum on log W *vs.* log c curve	D *vs.* log c curve
SDeS	3.80×10^{-4}	7.42×10^{-4}	2.46×10^{-4}
SDS	2.35×10^{-5}	5.25×10^{-5}	1.29×10^{-5}
STS	5.70×10^{-6}	1.26×10^{-5}	3.98×10^{-6}
SDSO	5.13×10^{-5}	8.32×10^{-5}	3.24×10^{-5}
SDBSO	1.15×10^{-5}	2.40×10^{-5}	6.92×10^{-6}
Manoxol OT	5.00×10^{-6}	9.33×10^{-6}	3.24×10^{-6}
DHP	1.82×10^{-5}	2.40×10^{-5}	4.91×10^{-6}

2. Measurement of ζ Potential by Electrophoresis

As was shown in Part 1, the important factor in the coagulation of hydrophobic sols by surface active agents is the change produced in surface potential rather than the change in ionic strength. This mechanism probably applies also for coagulation using trivalent citrate ions. Although it is not possible at the moment to measure the surface potential experimentally, the ζ potential is probably related closely to ψ_δ, and under certain conditions we can take $\psi_\delta \cong \zeta$. Thus, measurements of ζ potential provide up to a point a useful method for testing the derived theory of coagulation.

(i) ζ Potential of Positive Silver Iodide Sol Particles in the Absence of Surface Active Agents

Compared with the negative silver iodide sol, the readings of mobility measurements are more scattered, and hence the accuracy of measurement is lower. The ζ potential of the sol particles used in the experiments (pAg $=3$, $\tau=1.23$) was calculated from the experimental value of $U=4.7\mu$/sec/volt/cm, by using equation (12), giving the value $\zeta=140$ mV. This value is very high compared with that obtained by other authors, *e. g.* 50 mV[18] or 43 mV[27]. The latter value was uncorrected for the relaxation effect and no attempt was made by either set of authors to remove silicate ions from the system. Recently, however, Mirnik *et al*[28]. have measured the mobility of silver iodide sol particles at various pAg values using an A. C. method. According to the mobility *vs.* pAg curve given by them, the mobility at pAg 3 is about 4.8μ/sec/volt/cm, which is in good agreement with the above value.

(ii) ζ Potential of Positive Silver Iodide Sol Particles in the Presence of Surface Active Agents

a. ζ *vs.* log c curves. In Fig. 16 and 17 are shown curves of ζ *vs.* log molar concentration for sulphates and sulphonates with different chain lengths, and in

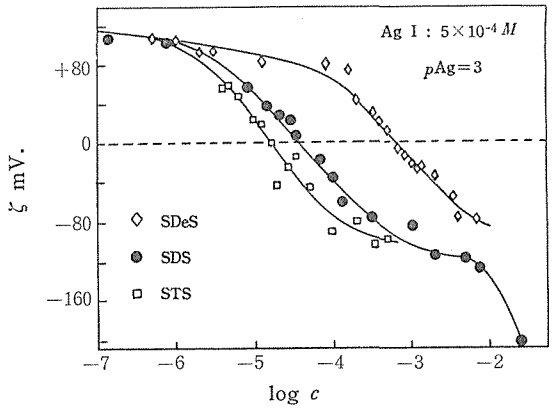

Fig. 16. ζ *vs.* log molar concn.

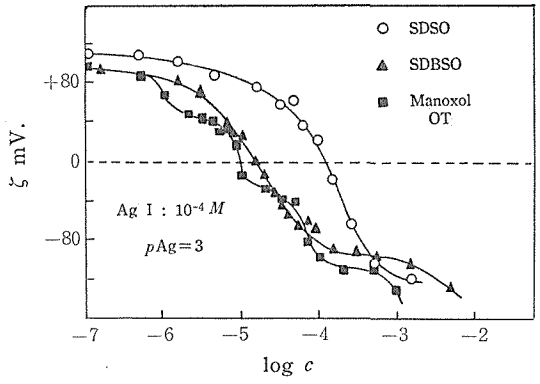

Fig. 17. ζ *vs.* log molar concn.

Fig. 18 curves for various dodecyl compounds with different head groups, *i. e.* sulphate, sulphonate and phosphate.

Generally, as the surface active agent concentration is increased the ζ potential remains practically constant until a certain concentration is reached, after which it gradually decreases to zero with increasing gradient, then reverses its sign and finally approaches a limiting negative value, which seems to differ for each surface active agent. If the concentration is increased further, the ζ value does not remain constant; an increase in negative potential occurs starting from near the critical micelle concentration (c. m. c.). This can be seen on the curves for SDS, SDBSO and Manoxol OT.

b. Effects of chain length and head group size variation. It is apparent from Fig. 16 that the ζ *vs.* log c curves for alkyl sulphates are almost parallel to each other and that the position of the curve shifts to lower concentrations for longer chain lengths. The same situation seems to hold also in the case of alkyl sulphonates, with the exception of Manoxol OT (Fig. 17).

On the other hand, for the same chain length the slopes of the ζ *vs.* log c curves are different for different head groups (Fig. 18). The ζ *vs.* log c curves cross the $\zeta=0$ line at different points and appear to converge to almost the same negative value of ζ at high concentrations before another steep increase (in the negative

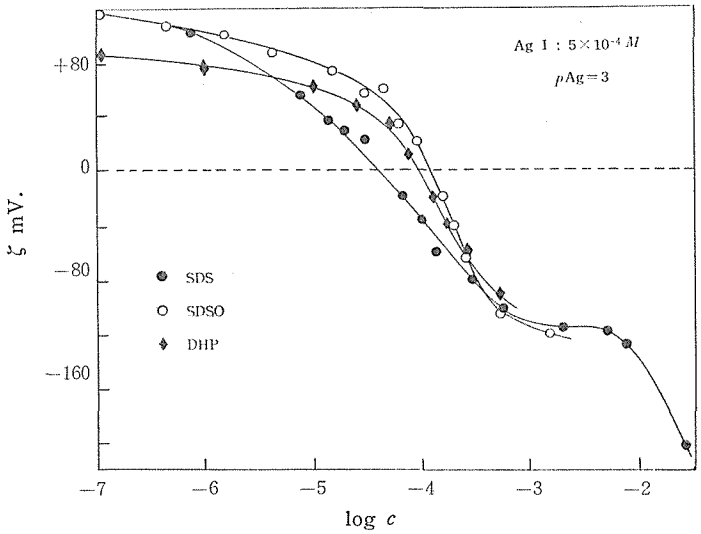

Fig. 18. ζ *vs.* log molar concn.

direction) occurs near the c. m. c.

The curve for Manoxol OT shows a rather complicated behaviour. It is very much like the curve obtained by Rastogi[10] using a negative silver iodide sol in the presence of bis-pyridinium decane bromide. These compounds appear to have a complicated mechanism of adsorption on the silver iodide surface, which is probably connected with the branched structure of the chain in the former case and with the presence of charged head groups at both ends of the alkyl chain in the latter.

c. Evaluation of N_1 and k_2. Except for the case of Manoxol OT, the ζ *vs.* log c curves appear to be of the general shape predicted by the theory developed in Part 1. Hence, by assuming that a single layer adsorption of the surface active agent is taking place up to the zero point of ζ, we can determine the values of the maximum number of available sites N_1 and the adsorption constant k_2 from equations (53) of Part 1[1]. By substituting $\psi_\delta=\zeta$ and $z=-1$, we obtain

Table 3. Parameters for adsorption of anionic surface active agents on positive silver iodide sols.
$\zeta^*=0.140$ volt, $\tau=1.23$, $a=10^{-6}$ cm, $\varepsilon=80$.

Surface active agent	$\left(\frac{d\zeta}{d\log c}\right)_{\zeta=0}$ volt	c° M	N_1 cm^{-2}	k_2 litre/M	c. m. c. in water at 25°C M
SDeS	−0.096	3.98×10^{-4}	1.94×10^{13}	6.80×10^{3}	3.6×10^{-2} [29]
SDS	−0.096	4.21×10^{-5}	1.94×10^{13}	6.41×10^{4}	7.6×10^{-3} [29]
STS	−0.096	1.68×10^{-5}	1.94×10^{13}	1.61×10^{5}	2.3×10^{-3} [29]
SDSO	−0.182	1.20×10^{-4}	2.91×10^{13}	7.93×10^{3}	8.5×10^{-3} [30]
SDBSO	−0.144	1.45×10^{-5}	2.48×10^{13}	9.17×10^{4}	1.2×10^{-3}** [31]
Manoxol OT	−0.182	9.50×10	—	—	—
DHP	−0.136	9.50×10	1.62×10	7.35×10	—

** at 60°C.

$$\left(\frac{d\zeta}{d\log c}\right)_{\zeta=0}=2.303\left[\frac{\zeta^*\varepsilon(1+\tau)}{4\pi aeN_1}-1\right] \tag{15}$$

and

$$\frac{1}{c^0}=k_2\left[\frac{4\pi aeN_1}{\zeta^*\varepsilon(1+\tau)}-1\right] \tag{16}$$

In Table 3 values of the various parameters, calculated from the experimental data of the ζ *vs.* log c curves by using equations (15) and (16), are given. For comparative purposes the c. m. c. values of the various surface active agents in water are given, where available. For materials of the same head group the value of k_2 appears to increase fairly regularly as the c. m. c. value decreases.

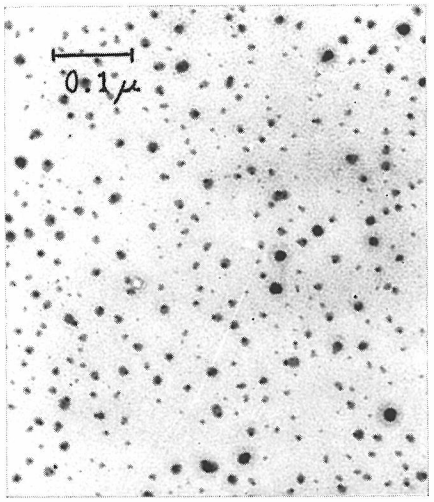

(A) 1 min after preparation,

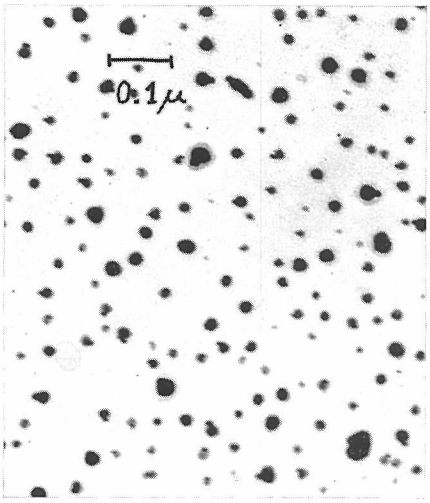

(B) 60 min after preparation,

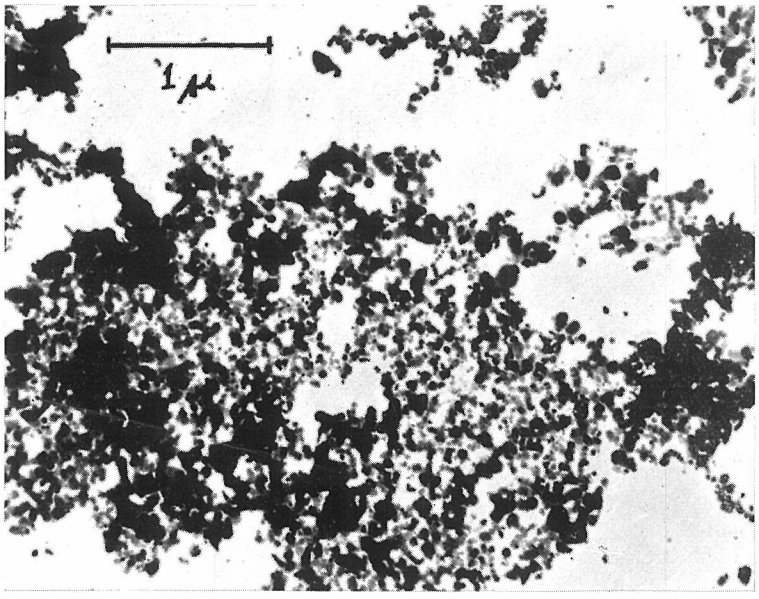

(C) Coagulation; 45 min after addition of SDS ($2\times10^{-5}M$).

Fig. 19 Electron micrographs of positive silver iodide sol particles. pAg=3.

3. Electron Micrographs

In Fig. 19 some of the electron micrographs are shown. Micrographs (A) and (B) are for the original positive silver iodide sol (pAg 3), and show the effect of ageing. The former was taken 1 min and the latter 60 min after preparation of the sol. It is clear that the particle grows considerably during this period; for particle size distribution see Fig. 2.

The micrograph (C) shows the effect of SDS in the coagulation concentration range and was taken 45 sec after addition of this surface active agent (final concentration of SDS was $2\times10^{-5}M$). This shows how the coagulation process occurs and the large clusters of particles which are formed.

IV. DISCUSSION

1. Turbidity Behaviour

(i) Coagulation by Inorganic Electrolytes

For the coagulation mechanism of double layer compression the slope of the log W *vs.* log c_e curves can easily be derived by using the Reerink-Overbeek equation (13), as[13]

$$\frac{d\log W}{d\log c_e} = -\frac{A}{24\,u_m\,kT} = -2.15\times10^{7}a\gamma^2/v^2 \qquad (13A)$$

with

$$u_m = Aev^2/(5.58\times10^{-5}a\gamma^2) = 1/\tau$$

and

$$\gamma = [\exp(v\,e\,\psi_\delta/2\,kT)-1]/[\exp(v\,e\,\psi_\delta/2\,kT)+1] \qquad (13B)$$

We can, therefore, calculate the values of the van der Waals constant A and the Stern potential ψ_δ from the experimental values of $d\log W/d\log c_e$ by using these equations. The values of A in Table 4 thus obtained are of the expected order of magnitude[12], whereas those of ψ_δ are a little lower than expected from experimental values of ζ potential since in general ψ_δ is larger than ζ. The analysis breaks down in the case of the citrate ion, since $(1+\gamma)/(1-\gamma)$ becomes negative. This again suggests that the mechanism of coagulation with citrate ions is different from the mechanisms by the other two anions; the coagulation occurs by the change in Stern potential rather than the double layer compression.

Table 4. Values of A and ψ_δ by the method of Reerink and Overbeek. Positive silver iodide sol, pAg=3, a=100 Å.

Electrolyte	$d\log W/d\log c_e$	A erg	ψ_δ mV
KNO_3	−4.20	0.8×10^{-12}	48
Na_2SO_4	−3.25	1.1×10^{-12}	52
Na_3 citrate	−4.35	—	—

(ii) Coagulation by Surface Active Agents

a. Sigmoid curves. The sigmoid type of curve has also been observed in

positive sol formation in the presence of anionic surface active agents (see Part 6), as well as in negative sol formation in the presence of cationic surface active agents[25]. One of the important features of this phenomenon is the fact that this type of induction period is strongly dependent on the particle size, see previously.

One possible explanation is as follows; the initial process of the reaction is crystal growth. This process is followed by the usual coagulation which gives rise to a much larger change in optical density. This means that, even if the surface concentration of the surface active agent, and hence the surface potential, remains the same, the particle must attain a certain size before coagulation can take place. In fact, it was observed by Rastogi[10] that the larger negative silver iodide sol is more unstable than the smaller one in the presence of cationic surface active agents.

Although the phenomenon can be explained in this manner, some experimental facts must be considered before a definite conclusion can be drawn. In the case of the precipitation of anionic surface active agents by cations the two processes of crystal growth and coagulation could under some conditions be distinguished by electron microscopy (Part 5). Moreover, the values of log W calculated from the slope of the second stage of the D *vs.* t curves agree with those expected theoretically; this may be considered to give an indirect proof of the present explanation.

b. Stability as a function of the surface active agent concentration. The experimental curves show a marked resemblance to the theoretical curves given in Fig. 5 in Part 1; the coagulation concentration range obtained experimentally is of almost exactly the predicted breadth and is broadened by a general increase in ionic strength. It is of interest that the curves obtained are broader than those obtained by Rastogi[10] in the coagulation of negative silver iodide sols by cationic surface active agents, where $\tau=0.66$ and $a=200$Å. In Table 5 a comparison is made between the theoretical and experimental values of d log W/d log c, *cf.* equation (59) of Part 1[1]. At log $W=2$, in the two cases where a comparison can be made, the experimental slopes are in good agreement with the theoretical value, but at log $W=1$ the experimental values are all smaller than the theoretical value. This is due to the improper value of A used for the calculation, *i. e.* 10^{-12} erg, and a better agreement is obtained by choosing a proper value for A.

It has already been pointed out that the experimental values of log W are smaller than those expected from the theory at high surface active agent concentrations. As the theory is based essentially on the assumption of single layer adsorptions, we can expect better agreement between theory and experiment at lower surface active agent concentrations. However, the introduction of the concept of second layer adsorption (see later) would still not explain the results obtained, because it would give higher values of surface potential than single layer adsorption in this range of surface active agent concentration, thus giving rise to higher stability.

Rastogi[10] has ascribed a similar phenomenon of decreasing stability at higher surface active agent concentrations, which occurred to a higher degree in coagulation of negative silver iodide sols, to the mutual coagulation between premicellar particles of surface active agents and the oppositely charged silver iodide particles. In fact Mukerjee *et al*[32]. have given evidence of the presence of dimers at concentration of SDS well below the c. m. c, *i. e.* at the concentration of about $10^{-4}M$. As this is

the region where the stability starts to fall for the second time, it would seem to justify the above interpretation of the decrease in stability at high surface active agent concentrations. This phenomenon does not occur with SDeS, since this material has much less tendency to form associated molecules than the other materials.

Table 5. Theoretical and experimental values of $d \log W/d \log c$. $\tau=1.23$, $A=10^{-12}$ erg.

$\log W$	$d \log W/d \log c$						
	Theoretical	Experimental					
		SDeS	SDS	STS	SDSO	SDBSO	Manoxol OT
2	21	—	—	21	20	—	—
1	20	6.4	5.5	8.0	6.6	6.0	8.6

2. Adsorption Behaviour of Surface Active Agents

(i) First Layer Adsorption The values of N_1 and k_2 obtained from the experimental data (Table 3) give useful information about the adsorption mechanism of surface active agents in the first layer.

We can assume that the initial adsorption of anionic surface active agents takes place at positive surface sites on the silver iodide particles, probably at points on the surface, occupied by potential determining silver ions. However, it is clear, from the fact that the ζ *vs.* $\log c$ curves cross the zero point of ζ, that the maximum number of sites is greater than the number of the excess silver ions on the surface; hence, the adsorption can take place on other sites as the concentration is increased. The values of N_1 in Table 3 show that this quantity is mainly determined by the nature of the negative head groups and appears to be independent of the length of the alkyl chain. In Table 6 the area occupied by a molecule, when all of the available sites of the first layer are occupied by surface active anions, is given. The values are about ten times greater than the areas occupied by a head group. This seems not unreasonable if the chains of the adsorbed surface active ions tend to lie parallel to the surface (see Part 4).

On the other hand, the adsorbability as measured by k_2 is mainly dependent on the oleophilic nature of the chain, and the longer the chain the larger is the value of k_2. It can be seen from the values of k_2 for different head groups (Table 3), that there is also fairly good agreement between SDS, DHP and SDBSO (the same alkyl chain group). On close inspection, however, there is a definite trend and the differences are larger than experimental errors. A much more marked deviation can be found in the case of SDSO; the value of k_2 is about 10 times smaller than the values for the other three of the same chain length.

Although the adsorbability of these materials is primarily due to the oleophilic character of chain groups, it will probably also be dependent on the character of head groups, *e.g.* such features as hydration, polarisability, *etc.* These factors will determine the "bond strength" between the head group and the silver ion on the

surface. Thus the interaction will depend also on the nature of the inorganic ion in the surface, and leads to a method for examining the interaction between surface active agents and various inorganic surfaces. The bond on the surface should be related to the strength of the bond formed between the single inorganic ions (*i. e.* in free solution) and the surface active agents; for example, ions with greater interaction will lead to precipitation of an insoluble salt. This concept will be extended in more detail in Part 3, where the counter ion binding of silver iodide surfaces covered with surface active agents will be discussed.

The chemical free energy of adsorption ΔG can be calculated from k_2 by using the equation (42) in Part 1[1], as

$$\Delta G = \Delta \bar{G} = -kT(\ln k_2 + \ln 55.6) \tag{17}$$

since at the zero point of ζ the electrical contribution becomes zero. In Table 6 the values of ΔG thus obtained are given.

Table 6. Free energy for the first layer adsorption of anionic surface active agents on positive silver iodide sols.

Surface active agents	Area/molecule sq. Å	$-\Delta G$ cal/mole
SDeS	516	7,560
SDS	516	8,880
STS	516	9,410
SDSO	344	7,650
SDBSO	404	9,080
DHP	617	8,940

(ii) Second Layer Adsorption

a. ζ Potential at high surface active agent concentrations. If we assume that first layer adsorption takes place in the whole concentration range of surface active agents, then the ζ *vs.* log c curve should tend to a negative limiting value which would be independent of k_2 but dependent on N_1. The limiting value, ζ^∞, can be derived by taking $k_2 c \gg 1$ in equation (48) of Part 1, assuming τ remains constant, *viz.*

$$\zeta^\infty = \zeta^* + k_1 = \zeta^* \left[1 - \frac{4\pi a e N_1}{\zeta^* \varepsilon (1+\tau)} \right] \tag{18}$$

$$\left(= -\zeta^*/k_2 c^0 \right)$$

In Table 7 the theoretical values of ζ^∞/ζ^* calculated from this equation using the parameters in Table 3 are given together with the corresponding experimental values. On comparing the theoretical and experimental values, we find that the agreement is very poor and that, as expected due to neglecting second layer adsorption, our theory no longer holds in this concentration range.

Again this discrepancy cannot be due to the assumption made with regard to the constancy of k_2, because the value of ζ^∞/ζ^* is independent of k_2 and only dependent on N_1; N_1 is again independent of k_2, *cf.* equation (15). We must, therefore, introduce another mechanism of adsorption in addition to the first layer adsorption

Table 7. Limiting values of ζ potential at high concentration of surface active agents.

Surface active agent	ζ^{∞}/ζ^{*}	
	Theoretical	Experimental
SDeS	−0.37	—
SDS	−0.37	−0.82
STS	−0.37	−0.71
SDSO	−1.06	−0.86
SDBSO	−0.75	−0.70
DHP	−0.14	(−0.77)

in order to explain this; that is, a different value of N_1 is necessary to explain the adsorption in the negative region, thus leading directly to a concept of second layer adsorption.

If we consider the structure of the double layer in this concentration range, it is more likely that additional surface active agent will be adsorbed on the surface with its negative head group directing towards the solution, because of the net negative charge at the inside layer and the van der Waals force between alkyl chain groups (see Part 4)[33]. This means that adsorption in the second layer is taking place with different values of N_1 and k_2 from those of the first layer. Whether the second layer adsorption starts to take place before the zero point of charge or not will probably depend upon the relative magnitude of ΔG of these two mechanisms. It seems from the values in Table 7 that the second layer adsorption commences to occur before the zero point of ζ in the case of alkyl sulphonate, because the experimental value of ζ^{∞}/ζ^{*} is smaller than the theoretical one; that is, the value of N_1 calculated on the basis of single layer adsorption might be an over-estimation. Another point to be considered here is the fact that in absolute value ζ potential is always smaller than ψ_δ potential, except when $\psi_\delta=0$. Hence, this gives rise to some uncertainty in the discussion of adsorption phenomena based upon ζ potential measurements.

The experimental values of ζ^{∞}/ζ^{*} in Table 7 have been obtained from the limiting values of ζ potential; that is the value just before the rapid negative increase of ζ potential which occurred near the c. m. c. Hence, in the extremely high concentration range, another adsorption mechanism of the anionic surface active agent must be considered to explain the rapid increase in ζ. This would probably involve the adsorption of highly charged micelles or premicelles, giving a high negative surface charge to the positive silver iodide particle, *i. e.* polylayer adsorption.

b. Evaluation of N_1' and k_2' for second layer adsorption. The additional adsorption of surface active agents in the second layer can be taken into account by adding an extra Langmuirian term[34] in equation (48) of Part 1, *viz.*

$$\zeta=\zeta^{*}+\frac{k_1 k_2 c}{1+k_2 c}+\frac{k_1' k_2' c}{1+k_2' c} \tag{19}$$

where

$$k_1'=4\pi z a e N_1'/[\varepsilon(1+\tau)]$$

and N_1' and k_2' are corresponding constants for the second layer. Here an approximation has been made by putting $\psi_\delta = \zeta$.

Before carrying out the calculation, some comment must be made here on equation (19).

It seems at first sight that this equation is based on the assumption of the two independent adsorption mechanisms. However, the second layer adsorption will probably take place on the long chain group of the surface active agents which are adsorbed in the first layer, due to the van der Waals forces between the chain groups. Hence, it will be strongly dependent on the extent of the adsorption in the first layer, although the latter can be considered to be independent of the former as a first approximation. This dependence can be taken into account, at least formally, by considering N_1' and k_2' as functions of $k_1 k_2/(1+k_2c)$.

Secondly, we must use the values of N_1 and k_2, which have been obtained by assuming the absence of the second layer adsorption, in order to estimate the values of N_1' and k_2'. This point is, no doubt, contradictory in a rigorous sense; the values of N_1 and k_2 obtained may be some average values including the effect of the second layer adsorption. However, second layer adsorption probably does not start to occur much before the zero point of charge. For example, in the case of STS, the value of k_2' is an order of magnitude smaller than k_2; this suggests that concentration ranges of the two mechanisms are fairly well separated.

It is clear from the above discussions that it may not be very accurate to estimate the values of N_1' and k_2' by using equation (19). However, at least these will give an approximate idea of the mechanism taking place in the second layer. As an example we shall consider the adsorption of STS. From the experimental data, we obtain $\zeta = -0.099$ and -0.089 volt for $c = 10^{-3}$ ($\tau = 1.58$) and $10^{-4}M$ ($\tau = 1.23$), respectively. Substituting these values and also $k_2 = 1.61 \times 10^5$, $N_1 = 1.94 \times 10^{13}$ and $\zeta^* = 0.140$ in equation (19), we obtain a set of equations with two unknowns, *i. e.* N_1' and k_2'. On solving these the following solutions are obtained:

$$N_1' = 8.75 \times 10^{12} \quad \text{cm}^{-2} \tag{20}$$

and

$$k_2' = 9.33 \times 10^3 \quad \text{litre}/M. \tag{21}$$

The electrochemical free energy of adsorption of the second layer can be calculated by using k_2', as

$$\Delta \bar{G}' = -7{,}740 \quad \text{cal/mole}$$

and the corresponding chemical free energy is calculated by substituting $\psi_\delta \cong \zeta = 0.089$ volt in equation (42) of Part 1, as

$$\Delta G' = -5{,}655 \quad \text{cal/mole} \tag{21A}$$

Although strictly speaking the separation of $\Delta \bar{G}'$ into electrical and chemical terms is not permitted[41], because ΔG itself also changes with ζ, *vide* Part 4, the above calculation gives an approximate order of magnitude of the free energy of adsorption in the second layer. Compared with the value of ΔG in Table 6, *i. e.* 9,410 cal/mole, the chemical free energy of adsorption in the second layer is about 4,000 cal smaller than that in the first layer. On the other hand, the maximum number of available

sites is not widely different from that of the first layer. This seems to show that the adsorption sites of the second layer are the long chains of the surface active agents adsorbed in the first layer. It is of interest, in this connexion, that the value obtained by Mukerjee *et al*[32]. for the formation of a dimer of SDS is about 3,000 cal/mole. Allowing for the fact that STS has two additional methylene groupings we can expect that the value of $\Delta G'$ obtained above is probably very close to that for formation of a dimer of STS; this provides direct evidence for the formation of dimers of anionic surface active agents, by association of the chains, on the silver iodide surface.

c. Thermodynamic consideration of the adsorption process of the anionic surface active agents. It has been shown that the experimental results of ζ potential measurements in the presence of anionic surface active agents could, in general, be explained by the decrease of the charge on the Stern plane with increasing surface active agent concentrations. If this is true, we come to a very useful conclusion. The original silver iodide surface can be considered as a non-polarisable electrode, because this surface is reversible to iodide ions and the Galvani potential difference ($\Delta\phi$) between the bulk phases of silver iodide and solution is completely determined by the iodide (or silver) concentration in the solution phase[35].

As the electrode potential of a silver-silver iodide electrode gives the Galvani potential difference, we can easily test experimentally whether the above description is true or not in the case of surface active iodide solutions. Fig. 20 shows the results

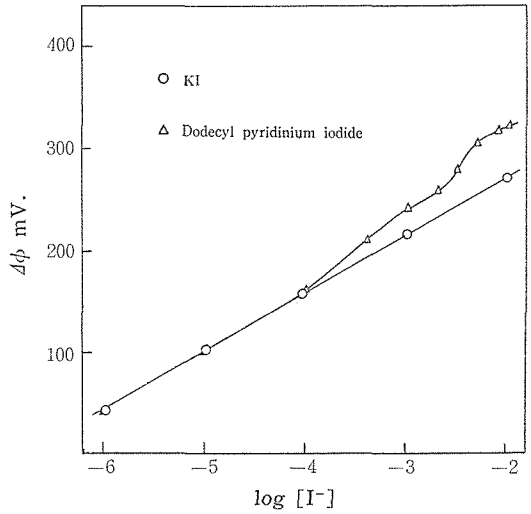

Fig. 20. Galvani potential difference of a rotating Ag—Ag I electrode as a function of the iodide concn. Ref. electrode: S. C. E.

of electrode potential measurement, using a silver-silver iodide electrode, in dodecyl pyridinium iodide solutions. It is clear from this experiment that the electrode potential ($\Delta\phi$) is a linear function of log iodide concentration up to and above the concentration where the ζ potential of silver iodide particles changes its sign. The slope of the experimental line is about 60 mV, which is in good agreement with the theoretical value of kT/e.

Although it is clear from thermodynamic considerations that, provided reversibility is maintained, this Galvani potential difference is dependent only on the bulk properties of the two phases, *i. e.* activities of iodide ions in both phases, the surface potential itself is strongly dependent on the state in the double layer. As long as there remains a sufficient number of available sites for adsorption of silver (or iodide) ions on the surface of the silver iodide particles, other silver (or iodide) ions are adsorbed to maintain equilibrium between the silver (or iodide) ions in the adsorption layer and in the solution, even if some adsorbed silver ions are coupled by surface active anions. Hence, there is no change in the net charge of the particle, and therefore no change in ψ_δ either. This is schematically shown in Fig. 21, (A) and (B).

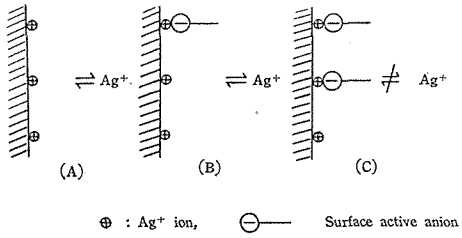

Fig. 21. Schematic representation of the reversibility of the potential determining process on Ag I surfaces.
(A) Clean surface (B) Small adsorption of S. A. A.
(C) Medium adsorption of S. A. A.

As the ζ potential behaviour in the second stage, *i. e.* the concentration range where a marked change in ζ occurs, could be explained by a Langmuir type of adsorption with reasonable values of N_1 and ΔG, it is strongly suggested by these electrode potential measurements that here the reversibility does not hold any more and the net surface charge starts to decrease with increasing surface active ion concentration, *vide* Fig. 21 (C).

The above description can be elaborated as follows; in the first stage the surface behaves as an ideal non-polarisable electrode. However, in the second stage it no longer follows this ideality and gradually changes to an ideal polarised electrode after the surface coverage has reached a certain value.

The condition of an ideal polarised electrode is the very slow rate of the potential determining process[35]. This is fulfilled by the fact that the coverage by surface active ions gives rise to a large potential barrier for the adsorption of potential determing silver ions. This is, of course, not completely fulfilled until all the surface silver ions are covered, and up to this concentration of surface active agent the surface behaves as a partially polarised electrode. We shall, therefore, treat the surface after the reversal of charge point is attained as an ideal polarised electrode.

One of the differences between the ideal polarised and the ideal non-polarisable electrodes is the existence of an extra degree of freedom in the former case. In our case this corresponds to the change in surface charge density of the ψ_δ-plane, and hence the ζ-potential, by changing the surface active agent concentration.

This may seem at first sight somewhat contradictory to the definition of ideal

polarisability, because the charge on the surface is determined by the reversible adsorption-desorption process of surface active agents. However, it makes no difference at all whether we change the surface charge by adsorption of surface active ions or by applying a potential difference from an external circuit, as is usual in the case of ideal polarised electrodes, *e. g.* mercury[36,37]. The surface charge density is an independent variable determined by the surface active agent concentration in the former case, and by the applied electromotive force in the latter.

These considerations on the properties of the silver iodide surface protected with surface active ions automatically leads to the conclusion that the surface, which we are really interested in from the view point to coagulation, is the ψ_δ-plane; that is, the plane from which the diffuse double layer starts towards the bulk of solution, rather than the inner plane on the surface of silver iodide particles. We can, therefore, treat the ψ_δ-plane as an ideal polarised electrode without considering any kind of potential determining ions, and we only need to consider the double layer extending from this plane into the bulk of solution.

This conclusion is very important for both theory and application. It is only mercury, and very rarely gallium, surfaces which have been studied as ideal polarised electrodes, because electrocapillary phenomena have been restricted to the study of conducting liquid metals[36,37]. Our conclusion shows the possibility of extending the range to cover various kinds of anionic and cationic surfaces, thus enabling the study of adsorption mechanisms of a much wider variety of combinations of adsorbents and adsorptives than before. An attempt of this kind of study is described in Part 3.

3. Stability and Surface Potential

(i) Observation of Coagulation in the Ultramicroscope Field

If the values of the coagulation concentration and c^0, in Tables 2 and 3, are compared, we find an intimate relation between them, thus justifying the basic idea of our theory that coagulation is due to the surface potential decrease by adsorption of surface active agents. In fact, small clusters of particles could be seen under the microscope during the mobility measurements in the range of small potentials. At concentrations where slow coagulation was taking place, we could find particles apparently sticking together, or at least moving in the direction of the electrical force as couples. As the surface active agent concentration was increased, 3- or 4-fold particles were observed, and very large clusters were found in the rapid coagulation range. At high surface active agent concentrations, *i. e.* in the stabilized region, a very finely dispersed sol was observed and the particle size appeared to be very small; this may be due to the change in refractive index of particles.

Although these observations were very qualitative, they give a rough idea of the process taking place. A similar effect was also encountered in the study of the binding of inorganic cations to silver iodide particles covered with surface active agents (Part 3)[38].

(ii) Log W *vs.* ζ Curves

The above idea can be discussed in a quantitative manner by considering the

relation between stability and surface potential. As we have obtained relations between log W and log c, and ζ and log c, we can now construct log W *vs.* ζ curves, and thus examine further the theory developed in Part 1.

In Fig. 22 and 23 are shown curves of log W *vs.* ζ of alkyl sulphates and sulphonates, respectively, and in Fig. 24 are given the curves for dodecyl compounds with different head groups. The dotted curve in each figure is the theoretical curve calculated from equation (33) by taking $\tau=1.23$ and $A=3\times10^{-12}$ erg.

It is clear that, although almost all the curves are shifted with respect to the ζ-axis, *i. e.* minimum W does not always occur at $\zeta=0$, and the minimum values of log W are not always zero, the shape of each curve is in good agreement with the theoretical curve, which is considered to hold for the range of ζ values from 25 to about 40 mV. It is a remarkable fact that even in the case of Manoxol OT, where

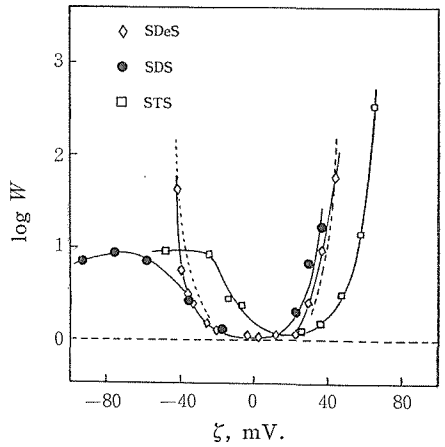

Fig. 22. Log stability *vs.* ζ.
Dotted lines: theoretical curves for $A=3\times10^{-12}$.

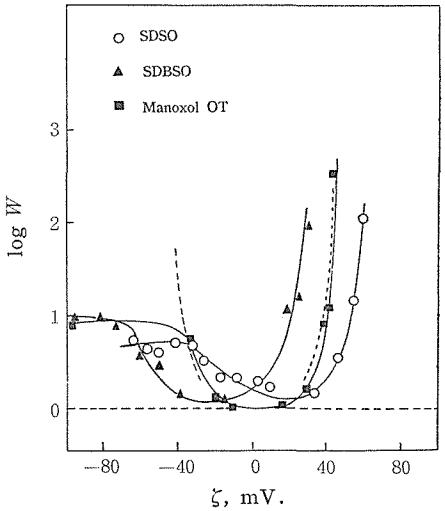

Fig. 24. Log stability *vs.* ζ.
Dotted lines: theoretical curves for $A=3\times10^{-12}$.

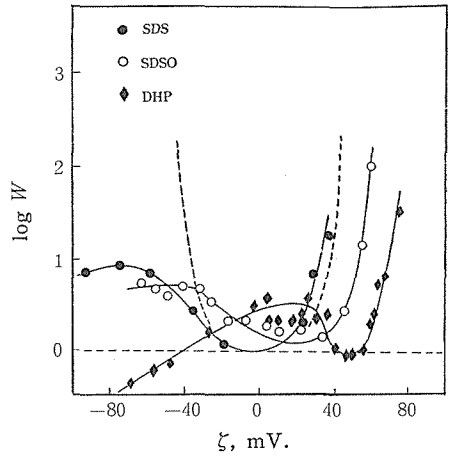

Fig. 24. Log stability *vs.* ζ.
Dotted lines: theoretical curves for $A=3\times10^{-12}$.

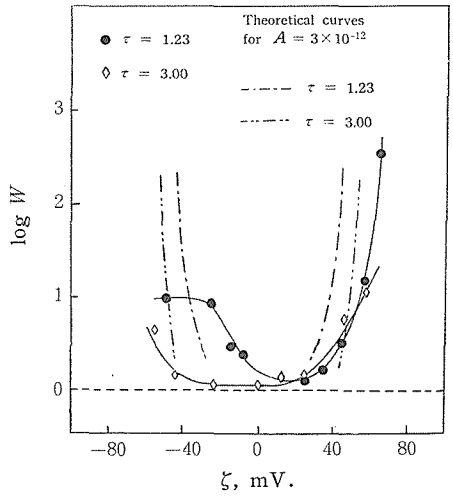

Fig. 25. Log stability *vs.* ζ for STS at different ionic strengths of Ag I sols.

the ζ *vs.* log c curve has a peculiar stepped form, the experimental log W *vs.* ζ curve agrees with the theoretical curve, and moreover, the agreement seems to be better than with the other surface active agents. In the negative ζ potential range the experimental values of log W are lower than the theoretical values except in the case of SDeS. It has been previously shown that the lowered stability in this range could be explained on the basis of premicelle formation of surface active agents, and it is apparent that in the case of SDeS the c. m. c. is sufficiently high that this mechanism does not occur in this concentration range.

The validity of the theory can be checked further by examining the effect of changing τ on log W. In Fig. 25 are shown the log W *vs.* ζ curves obtained from coagulation and ζ potential measurements of positive silver iodide sols at two different values of τ, *i. e.* 1.23 and 3.00. In the same figure are plotted the correspond-

ing theoretical curves calculated from equation (34) of Part 1 with $A=3\times10^{-12}$ erg. Although the agreement between the experimental and theoretical curves is not so good as compared with the cases shown before, it is clear that the effect of increasing τ is to decrease stability for the same value of ζ, in accord with the theoretical expectation.

(iii) Deviations of Experimental Results from Theory

The above discussion seems to show that the theoretical treatment of Part 1 is valid in principle, but there are a few definite deviations which must be considered.

Firstly, the agreement between theory and experiment is in general not so good in the negative region of ζ potential. *i. e.* at higher surface active agent concentrations. This has been discussed already, and ascribed to the mutual coagulation taking place between silver iodide particles and the premicelles of surface active agents, see previously.

Secondly, although the general shape of the log W *vs.* ζ curve shows excellent agreement with the theory, the curves are usually shifted in position; that is the minimum value of W is not always unity, and does not always occur at the zero point of ζ. Examination of log W *vs.* ζ curves shows that there seems to be a close relation between these deviations. That is, the minimum value of log W is higher for the surface active agent which shows larger deviation of ζ potential from the zero point. In Table 8 this deviation, ζ_{min}, and the minimum value, log W_{min}, are given. In the same table are also shown the surface charge density values at the minimum, σ_{min} by using the relation:

$$\sigma_{min}=(\varepsilon\,\zeta_{min}/4\pi\,a)(1+\kappa a) \qquad (22)$$

As the theory derived in Part 1 is in principle based on the change of Coulombic interactions between particles due to the surface potential, the stability factor, as a function of ζ, should be independent of the specific characteristics of the surface active agent used as the coagulating agent ; these characters are expressed in equation (34) of Part 1 only implicitly in terms of ψ_δ, or ζ. Therefore, the above

Table 8. Deviations of the stability minimum from ideality.

Surface active agent	log W_{min}	ζ_{min} volt	σ_{min} esu
SDeS	0.02	+0.015	$+7.06\times10^2$
SDS	0.02	−0.015	-7.06×10^2
STS	0.08	+0.020	$+9.42\times10^2$
SDSO	0.08	+0.020	$+9.42\times10^2$
SDBSO	0.06	−0.013	-6.12×10^2
Manoxol OT	0.00	+0.004	$+1.88\times10^2$
DHP	0.00	+0.000	0

mentioned deviation must be interpreted by introducing some kind of perturbation of the free energy of interaction between particles, which is related to the specific character of the surface active agent.

This perturbation can be expressed formally by postulating some remaining

potential barrier at the minimum point, which interferes with the free diffusion of the particles. If we represent this by an activation energy $\Delta F^{\neq}$ which must be overcome by the particles, the coagulation rate at the minimum, k_{min}, is given by

$$k_{min} = k_0 \exp(-\Delta F^{\neq}/kT)$$

where k_0 is the rate of rapid coagulation, *i. e.* equation (13A) of Part 1. Hence

$$\ln W_{min} = \ln (k_0/k_{min}) = \Delta F^{\neq}/kT = \mathrm{f}(\zeta_{min}).$$

It is rather difficult to determine the exact form of $\Delta F^{\neq}$ as a function of ζ_{min} from the experimental data in Table 8, because the absolute values of log W_{min} obtained are very small and a large error can easily be introduced. However these values seem to show qualitatively that the former is an increasing symmetric function of the latter, because the absolute value of ζ_{min} seems to determine the magnitude of $\Delta F^{\neq}$. This supposition is quite in accord with the theory of Part 1. That is, if we inspect equation (27) of Part 1 it can easily be seen that the potential term always appears in the form of ψ^2.

The fact that all of the log W *vs.* ζ curves can be superimposed approximately by shifting them in relation to the abscissa is analytically equivalent to making the following substitution:

$$\psi = \varphi(\zeta - \zeta_{min}), \quad \varphi > 1 \tag{23A}$$

where the factor φ has been introduced to take into account the fact that the plane of shear does not always coincide with the ψ_δ-plane. Here, the specific character of the surface active agent is introduced by the term ζ_{min}.

These deductions finally lead to the following equation:

$$\psi^2 = \varphi^2[(\zeta - \zeta_{min})^2 + b\,\zeta_{min}^2] \tag{23}$$

where b is an unknown constant.

Although equation (23) has been derived from the formal analysis of experimental results and does not give any physical picture of the process taking place, an attempt will be made in the Appendix to derive this equation by considering dipole interactions; this will probably become important when the distance of two approaching particles becomes very small.

The author takes pleasure in expressing his gratitude to Dr. R. H. Ottewill, University of Cambridge, for his kind supervision and continuous advice during the course of this work. Thanks are also due to the British Council for the Scholarship and to the University of Cambridge for the award of the Oliver Gatty Studentship. The author's thanks are also due to Dr. R. W. Horne, Cavendish Laboratory, for taking electron micrographs and to Imperial Chemical Industries, Dyestuffs Division, for supplying the SDeS, SDS and STS, the late Dr. A. V. Few for the SDSO, and SDBSO, Messrs. Hardman and Holden, Ltd. for Manoxol OT, and Dr. H. C. Parreira for the DHP. The author wishes also to express his gratitude to Professor I. Tachi and to Dr. S. Ueda for their continuous interest and encouragement.

APPENDIX

DIPOLAR INTERACTION BETWEEN TWO APPROACHING PARTICLES

(i) Theoretical Treatment

If one considers two particle surfaces 1 and 2, having the same charge density σ (taken to be positive) and a permanent dipole moment $\mathbf{m}$ per unit area, see Fig. A.1, and if the distance vector, $\mathbf{x}$, is taken from 1 to 2, the electric fields at 1 and

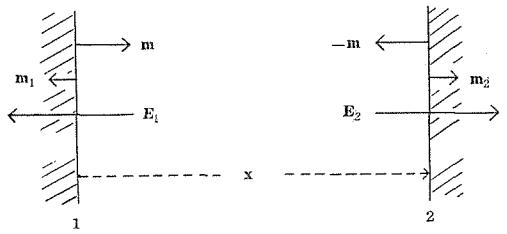

Fig. A. 1. Schematic diagram of two approaching particle surfaces.

2, $\mathbf{E}_1$ and $\mathbf{E}_2$, are given by[39],

$$\mathbf{E}_1 = -\frac{\sigma}{x^3}\mathbf{x} + \frac{2}{x^3}\mathbf{m}_2 - \frac{2}{x^3}\mathbf{m}$$

$$\mathbf{E}_2 = \frac{\sigma}{x^3}\mathbf{x} + \frac{2}{x^3}\mathbf{m}_1 + \frac{2}{x^3}\mathbf{m} \qquad \text{(A. 1)}$$

where $\mathbf{m}_1$ and $\mathbf{m}_2$ are respectively the dipole moments per unit area of surfaces 1 and 2 induced by the fields. On the other hand, these quantities are related to the polarisability of the surfaces, α, by the relation

$$\mathbf{m}_1 = \alpha\,\mathbf{E}_1 \quad \text{and} \quad \mathbf{m}_2 = \alpha\,\mathbf{E}_2 \qquad \text{(A. 2)}$$

By eliminating $\mathbf{E}_1$ and $\mathbf{E}_2$ from equations (A. 1) and (A. 2) we obtain

$$\mathbf{m}_1 = -\frac{\alpha(\sigma\mathbf{x}+2\mathbf{m})}{x^3+2\alpha}$$

$$\mathbf{m}_2 = \frac{\alpha(\alpha\mathbf{x}+2\mathbf{m})}{x^3+2\alpha} \qquad \text{(A. 3)}$$

where x is the modulus of the vector $\mathbf{x}$.

Now the resultant moments of the two surfaces, $\mathbf{m}_1^*$ and $\mathbf{m}_2^*$ are introduced by the following equations, *viz.*

$$\mathbf{m}_1^* = \mathbf{m}_1 + \mathbf{m}$$

$$\mathbf{m}_2^* = \mathbf{m}_2 - \mathbf{m} \qquad \text{(A. 4)}$$

The free energy of this system, F, is given by the work necessary to bring the two surfaces from $x = \infty$ to $x = x$, hence[39]

$$F = \frac{\sigma^2}{x} + \frac{1}{x^2}(\sigma m_1^* - \sigma m_2^*) - \frac{2m_1^* m_2^*}{x^3} + \frac{m_1^* + m_2^*}{2\alpha} \qquad \text{(A. 5)}$$

The first term in this equation represents the Coulombic, the second term the charge-dipole and the third term dipole-dipole interactions, and the last term is the

work necessary to induce the moments $\mathbf{m}_1$ and $\mathbf{m}_2$. Here the quantities expressed by the ordinary scripts are the moduli of corresponding vectors; m_1^* and m_2^* are taken to be positive if the directions of corresponding vectors are from 1 to 2, and *vice versa*.

The calculation of F is complicated, so a simple case, where $\mathbf{m}$ and $\mathbf{x}$ have the same direction except their signs, is considered in order to obtain an idea of the maximum correction for the free energy of interaction caused by the dipolar interactions.

The signs of m_1^* and m_2^* depend on the magnitudes of α, σ and m, but always $m_1^*=-m_2^*$, because $m_1=-m_2$, see equation (A. 3). For the moment it is assumed that $m_1^*>0$. After an elementary calculation, equation (A .5) reads

$$F=\frac{x^3+\alpha}{(x+2\alpha)\,x}\left(\sigma+\frac{mx^2}{x^3+\alpha}\right)^2+\frac{m^2}{x^3+\alpha} \tag{A. 6}$$

or

$$F=\frac{1+p}{(1+2p)\,x}\left[\sigma+\frac{m}{x}\cdot\frac{1}{1+p}\right]^2+\frac{m^2}{x^3(1+p)} \tag{A. 7}$$

where $p=\alpha/x^3$.

Equation (A. 7) can be rewritten as

$$F=q\frac{(\sigma+\sigma_{min})^2}{x}+\frac{\sigma_{min}^2}{x} \tag{A, 8}$$

where

$$q=\frac{1+p}{1+2p}\cong 1 \text{ and } <1 \tag{A. 9}$$

and

$$\sigma_{min}=\frac{m}{x}\cdot\frac{1}{1+p} \tag{A.10}$$

It is clear that equation (A. 8) has a form which is similar to that deduced from the experimental results in the text; *cf.* equation (23). This equation means that, if there are induced and permanent dipoles on surfaces, the mutual interactions between the field and these dipoles and the surface charges operate to shift the minimum point of the free energy by an amount proportional to the permanent dipole moment. At the same time, the minimum value is increased by an amount proportional to the square of the dipole moment, see Fig. A. 2.

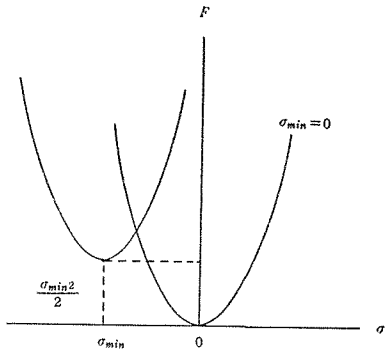

Fig. A. 2. Shift of the free energy minimum.

It is clear from the basic idea of the above derivation, that the free energy of the system may be given by

$$F=\sigma_{eff}^2/x \qquad (A.11)$$

if no interaction occurs other than that between charges. From equations (A.8), (A.9) and (A.11) we obtain

$$\sigma_{eff}=[(\sigma+\sigma_{min})^2+\sigma_{min}^2]^{1/2} \qquad (A.12)$$

In other words, the effective charge of the surface is increased by the presence of dipolar interactions and it is only when $m=0$ that σ_{eff} is equal to σ, *i.e.* the true charge density.

Although these equations are expressed in terms of the surface charge instead of the surface potential, the discussion applies also to the case expressed in terms of the surface potential ψ, since there exists a linear relationship between ψ_δ and σ in the range of major interest.

The above calculations were made for the case of positive **m**. In the case of negative **m**, we obtain, instead of equation (A.10),

$$\sigma_{min}=-\frac{m}{x}\frac{1}{1+p} \qquad (A.13)$$

The shift of the minimum point is in opposite direction from that described above. The term σ_{min}^2/x, however, does not change the sign. That is, the direction of the minimum point gives some idea about the direction of the permanent dipole moment of the surface.

It is clear that steric hindrance will also give rise to an increase in the free energy of interaction. This has been studied by Mackor and van der Waals[40].

(ii) Comparison with the Experimental Data in the Text

It is difficult at the moment to decide what is the origin of the dipole moment of the surface, but there are several possibilities which might give rise to an electrical moment at the surface.

a. The combination of the potential determining silver ion and the negative head group of the surface active agent. In this case the number of dipoles per unit area, n, is given by

$$n=\sigma_{min}/e$$

Hence, from equation (A.10), when p is small compared to unity, we obtain the moment of a single dipole, m', as

$$m'=ex$$

That is, it is impossible to estimate the value of m' from experimental value of σ_{min}.

b. Water dipole. If we put, arbitrarily, $x=2\times10^{-8}$ cm, $m'=1.6\times10^{-18}$ esu, *i.e.* the dipole moment of a water molecule, and $\sigma_{min}=9.42\times10^{2}$ esu, see Table 8, we obtain from equation (A.13)

$$n=1.19\times10^{13}\ \text{cm}^{-2}$$

or the area occupied by a single water dipole becomes 1000 Å^2. This value, for the area occupied, is too high and hence this model would appear to be inappropriate.

c. The electrical moment of the double layer. This can give rise to an electrical moment, and the effect of the chain length of the surface active agent is to decrease the dielectric constant of the equivalent condenser at the surface.

d. The dipole moment of the long chain. In the case of STS the stability minimum occurs at a concentration of *ca.* 10^{-5} *M*/litre, see Table 2, and hence the number of STS molecules adsorbed per unit area, n, is 1.19×10^{13} cm^{-2}. Therefore, we obtain

$$m' = (\sigma_{min}/n)x = 7.92\times10^{-11} \text{ esu}$$

In Table A.1 the values of m' corresponding to various values of x are given.

Table A. 1. Calculated dipole moment of the surface.

x, cm	m', Debye unit
20×10^{-8}	15.8
2×10^{-8}	1.58
1×10^{-8}	0.80

It can be seen that the value of m' is of the right order of magnitude for ordinary molecular dipoles, if we take the value of x to be 2×10^{-8} cm. This means that the effective dimension of the dipole of the chain is much smaller than the value expected from the chain length, *i. e. ca.* 20×10^{-8} cm. As this quantity is the component of the distance between two charges of the dipole perpendicular to the surface, the above calculation appears to suggest that the long chain group of the surface active agent is not perpendicular to the surface but almost parallel to it with very small angle.

This is not an unreasonable picture, because due to its hydrophobic character the long chain is more likely to be pushed out of the solution phase and on to the interface. The fact that the area occupied by the anionic surface active agents is about 500Å^2 also supports this picture.

REFERENCES

(1) A. Watanabe, This Bulletin, **38**, 158 (1960).
(2) H. R. Kruyt and S. A. Troelstra, *Kolloid Beih.*, **54**, 262 (1943).
(3) H. Freundlich, "Colloid and Capillary Chemistry," Methuen, London, p. 420 (1926).
(4) H. Freundlich, *Z. physik. Chem.*, **44**, 135 (1903).
(5) A. Lottermoser and R. Steudel, *Kolloid Z.*, **82**, 319 (1938) ; **83**, 37 (1938).
(6) J. F. Hazel and H. O. Strange, *J. Colloid Sci.*, **12**, 529 (1957) ; *J. phys. Chem.*, **61**, 1281 (1957).
(7) B. Tamamushi and K. Tamaki, *Kolloid Z.*, **163**, 122 (1959).
(8) K. Megro and T. Kondo, *J. Chem. Soc., Japan*, **76**, 642 (1955) ; T. Megro, *ibid.*, **77**, 77 (1956).
(9) B. Tamamushi, *Kolloid Z.*, **150**, 44 (1957).
(10) M. C. Rastogi, Ph. D. Thesis, Cambridge (1958).
(11) S. A. Troelstra and H. R. Kruyt, *Kolloid Beih.*, **54**, 225 (1943).
(12) R. H. Ottewill and J. A. Sirs, *Bull. Photoelectric Spectrometry Group*, **10**, 262 (1957).
(13) H. Reerink and J. Th. G. Overbeek, *Disc. Faraday Soc.*, **18**, 74 (1954).

(14) J. Lijklema, Doctoral Dissertation, Utrecht (1957).
(15) E. J. Verwey and J. Th. G. Overbeek, "Theory of Stability of Hydrophobic Colloids," Elsevier, Amsterdam (1948).
(19) J. A. W. van Laar, Doctoral Dissertation, Utrecht (1952).
(17) G. Oster, *J. Colloid Sci.*, 2, 290 (1947).
(18) S.A. Troelstra and H. R. Kruyt, *Kolloid Z.*, 101, 182 (1942).
(19) G. E. van Gils and H.R. Kruyt, *Kolloid Beih.*, 45, 60 (1937).
(20) K.N. Davies and A. K. Holliday, *Trans. Faraday Soc.*, 48, 1061, 1066 (1952).
(21) J. Th. G. Overbeek, *Kolloid Beih.*, 54, 287 (1943).
(22) Wiersma, private communication to R. H. Ottewill.
(23) R. W. Horne and R.H. Ottewill, *J. Phot. Science*, 6, 39 (1958) ; R. H. Ottewill and R. W. Horne, *Kolloid Z.*, 149, 122 (1956).
(24) H. C. Parreira, Ph. D. Thesis, Cambridge (1958).
(25) E. Matijević and R. H. Ottewill, *J. Colloid Sci.*, 13, 242 (1958).
(26) B. Težak, E. Matijević, K. F. Schulz, J. Kratohvil, M. Mirnik and V. B. Vouk, *Disc. Faraday Soc.*, 18, 63 (1954).
(27) G. N. Gorochowsky, *J. phys. Chem.*, 39, 465 (1935).
(28) M. Mirnik, F. Flašman and B. Težak, *Croatia Chemica Acta*, 28, 167 (1956).
(29) W. Prins, Doctoral Dissertation, Leiden (1955).
(30) E. L. McBain, W.B. Dye and S. A. Johnston, *J. Am. Chem. Soc.*, 61, 3210 (1939).
(31) R. G. Paquette, E.C. Lingafelter and H. V. Tartar, *J. Am. Chem. Soc.*, 65, 686 (1943).
(32) P. Mukerjee, K. J. Mysels and C. J. Dulin, *J. phys. Chem.*, 62, 1390 (1958) ; P. Mukerjee, *ibid.*, 1937 ; P. Mukerjee and K. J. Mysels, *ibid.*, 1400.
(33) A. Watanabe, This Bulletin, Part 4 (1960).
(34) J. T. Edsall and J. Wyman, "Biophysical Chemistry", 1, Academic Press (1958).
(35) R. Parsons, in Bockris', "Modern Aspects of Electrochemistry," 1, Butterworths, London (1954).
(36) D. C. Grahame, *Chem. Rev.*, 41, 441 (1947).
(37) A. Watanabe and S. Ueda, *J. electrochem. Soc., Japan*, 20, 247, 308, 358, 419 (1952).
(38) A. Watanabe, This Bulletin. 38, 216 (1960).
(39) C. J. F. Böttcher, "Theory of Electric Polarisation," Elsevier, Amsterdam (1952).
(40) E. L. Mackor and J. H. van der Waals, *J. Colloid Sci.*, 4, 425 (1949).
(41) E. A. Guggenheim, *J. phys. Chem.*, 33, 842 (1929).